Structural Insights into the Effect of Hydration and Ions on A-Tract DNA: A Molecular Dynamics Study

A. Madhumalar* and Manju Bansal*†
*Molecular Biophysics Unit, Indian Institute of Science, Bangalore 560012, India; and
†Institute of Bioinformatics and Applied Biotechnology, International Tech Park Ltd., Bangalore 560066, India

ABSTRACT DNA structure is known to be sensitive to hydration and ionic environment. To explore the dynamics, hydration, and ion binding features of A-tract sequences, a 7-ns Molecular dynamics (MD) study has been performed on the dodecamer d(CGCAAATTTGCG)$_2$. The results suggest that the intrusion of Na^+ ion into the minor groove is a rare event and the structure of this dodecamer is not very sensitive to the location of the sodium ions. The prolonged MD simulation successfully leads to the formation of sequence dependent hydration patterns in the minor groove, often called spine of hydration near the A-rich region and ribbon of hydration near the GC regions. Such sequence dependent differences in the hydration patterns have been seen earlier in the high resolution crystal structure of the Drew-Dickerson sequence, but not reported for the medium resolution structures (2.0 ~ 3.0 Å). Several water molecules are also seen in the major groove of the MD simulated structure, though they are not highly ordered over the extended MD. The characteristic narrowing of the minor groove in the A-tract region is seen to precede the formation of the spine of hydration. Finally, the occurrence of cross-strand C2–H2...O2 hydrogen bonds in the minor groove of A-tract sequences is confirmed. These are found to occur even before the narrowing of the minor groove, indicating that such interactions are an intrinsic feature of A-tract sequences.

INTRODUCTION

Sequence dependent conformational flexibility of DNA is of great interest due to its implications for drug-DNA and DNA-protein interactions. An understanding of the environment dependent sensitivity of DNA structure is necessary to elucidate its structure-function relationships. In particular the structure of A-tracts has been of interest for more than two decades, because of its apparently unique structural properties and the implication of this sequence in several regions of biological interest, including nucleosome structure, in which DNA curvature facilitates the formation of the solenoidal DNA-histone complex (Constanz et al., 1990), as loci for bent DNA in free form as well as complexes with regulatory proteins (El Hassan and Calladine, 1998), and as sites for minor groove binding drugs (Kopka et al., 1985; Quintana et al., 1991; Vega et al., 1994; Brown et al., 1990; Edwards et al., 1992; Laughton et al., 1996; Simpson et al., 2000; Clark et al., 1996a,b; Larsen et al., 1989; Goodsell et al., 1995; Brown et al., 1992; Tabernero et al., 1993; Cristina Vega et al., 1994; Spink et al., 1994; Nunn and Neidle, 1995; Coll et al., 1987).

The first crystal structure of B-DNA type oligomer, d(CGCGAATTCGCG)$_2$ (hereafter referred as A_2T_2), reported by Dickerson and co-workers (Drew and Dickerson, 1981), contained an A-tract, and it demonstrated that the minor groove size as well as other local parameters of DNA vary in a sequence dependent fashion. The minor groove was found to be narrower in the A-tract spanning region than in GC containing regions. Later, NMR (Liepinsh et al., 1992), chemical foot-printing (Burkhoff and Tullius, 1987), and computer modeling studies (Young et al., 1997a,b) on this sequence also supported this concept of sequence specific variation in local conformation. A critical question very much in focus in recent literature is whether conformational flexibility is influenced more by the sequence or by the environment, which includes the effect of hydration and bound cations. Many theoretical predictions from Molecular dynamics (MD) simulation (Young et al., 1997a; Feig and Pettit, 1999; Hamelberg et al., 2000; Bonvin, 2000; Hamelberg et al., 2001) and experimental observations from x-ray crystallography (Shui et al., 1998; Chiu et al., 1999; Tereshko et al., 1999a,b; Woods et al., 2000) and NMR (Hud et al., 1999; Hud and Feigon, 1997) supported the idea of a well-defined hydration pattern in the minor groove and fractional occupancy of cations within this hydration shell, in B-form DNA. On the other hand, recent reports from MD simulations on A-tracts (McConnell and Beveridge, 2000) and from NMR studies (Denisov and Halle, 2000) suggest that the structure of A-tract duplex is not highly sensitive to the presence of sodium ion in the groove. In addition, even the high resolution (1.1 Å) crystal structure of the A_2T_2 duplex did not provide any evidence for the presence of Na^+ ions in the minor groove (Tereshko et al., 1999a). However, other monovalent cations Tl^+ (Howerton et al., 2001), K^+ (Sines et al., 2000), Rb^+ (Tereshko et al., 1999b), Cs^+ (Woods et al., 2000), and NH_4^+ (Hud et al., 1999), and divalent cations Mn^{2+}(Hud and Feigon, 1997), Mg^{2+} (Tereshko et al., 1999a; Minasov et al., 1999), and Ca^{2+} (Minasov et al., 1999; Chiu and Dickerson, 2000), are reported to occur sometimes within the minor groove hydration shell.

Submitted December 18, 2002, and accepted for publication April 21, 2003.

Address reprint requests to Manju Bansal, Tel.: 91-80-293-2534 or 91-80-841-0029; Fax: 91-80-360-0535; E-mail: mbansal@ibab.ac.in or mb@mbu.iisc.ernet.in.

0006-3495/03/09/1805/12 $2.00

To investigate this further, a 7-ns MD study has been carried out on d(CGCAAATTTGCG)$_2$ (hereafter referred as A_3T_3) that contains a longer A-tract. This sequence serves as a preferential binding site for several drugs (Brown et al., 1992; Tabernero et al., 1993; Cristina Vega et al., 1994; Spink et al., 1994; Clark et al., 1996a,b; Nunn and Neidle, 1995) that bind to AT rich minor groove regions of the DNA duplex. Since the reason behind this preferential binding is believed to be the narrow minor groove in AT rich regions, it is necessary to understand in what order the two phenomena (groove narrowing and ion binding) occur. Earlier MD studies (1 ns each), on this sequence and other similar sequences, where one or more of the three A.T basepairs were mutated to ionosine.methylcytosine (Sherer et al., 1999), were mainly focused on studying the effect of A-tract sequence on DNA bending. However, the sequence dependent hydration patterns, the effect of monovalent counterions, and the structural features such as groove narrowing have not been discussed. Our longer MD study (7 ns) on the dodecamer containing A_3T_3 sequence provides several interesting insights into all the sequence dependent key features of the A-tracts, such as spine of hydration, narrow minor groove, as well as cross-strand C–H. . .O hydrogen bonds. The study also reveals the intrinsic sequence dependent nature of groove narrowing in the A-tract regions and seems to confirm that the presence of monovalent counterions does not appear to play a major role in defining their characteristic structural features.

METHODS

The MD simulation was carried out using AMBER5 with standard force field (Cornell et al., 1995). Coordinates of the 12-mer starting B-DNA model were generated using Nucgen module of AMBER5. The system was then neutralized by placing 22 Na^+ counterions at a distance of 6 Å from the phosphorous atoms. The system of DNA and counterions were immersed in the Monte Carlo equilibrated periodic TIP3P water bath, which extended up to a distance of 6 Å. The final system contained 2246 water molecules and the total number of atoms in the system was 7520.

The system of DNA, counterions, and water molecules was heated from 0 to 100 K while keeping large constraint of 1000 kcal/mol Å on the DNA atoms. An MD run of 10 ps was done for the above system. Then the system was slowly allowed to relax in 500 cycles of minimization. A 10-ps MD run was carried out, reducing the constraints on the DNA atoms to 500 kcal/mol Å. At this step the temperature of the system is slowly raised from 0 to 100 K in steps of 20 K. Then the constraints on the DNA atoms were reduced in steps of 250, 200, 100, 50, 25, 20, 10, and 5 kcal/mol Å. A 10-ps MD run was done for each of the above constraints. Thus the system was equilibrated for 100 ps, followed by full energy minimization. This method is similar to the one reported elsewhere (Shields et al., 1997).

After this initial equilibration the whole system was heated to 300 K in steps of 50 K. A 2-ps MD run was carried out for each step without positional constraints on the DNA atoms. The initial production run of 2 ns was carried out using the SANDER module of AMBER5. To facilitate greater rearrangement of water and ions, the system was heated to 400 K and an MD run of 1 ns was continued at this temperature. The system temperature was then brought down to 300 K in steps of 20 K and the simulation was continued for another 4 ns to a total duration of 7 ns. The entire simulation was carried out under NPT condition. Constant pressure and temperature conditions were maintained via Berendsen algorithms, with the coupling constants of 0.1 ps and 0.2 ps. The nonbonded cutoff of 9 Å was used for solvent-solvent, solvent-solute interactions and the Particle Mesh Ewald method was used for the calculation of long-range electrostatic interactions (Darden et al., 1993). The nonbonded pair list was updated every 25 steps and all the bonds were constrained using the SHAKE algorithm. The integration time step of 2 fs was used and the structures were stored after every 1 ps. All the structures were analyzed using NUPARM (Bhattacharya and Bansal, 1989; Bansal et al., 1995) and all the trajectory plots were created using the MATLAB package.

Crystallographic refinements

The ion and water coordination sites were determined using pseudocrystallographic refinement technique (Duan et al., 1997). This refinement was carried out for two sets of 100 snapshots, obtained from 1.5 to 2-ns and 6.5 to 7-ns ranges, taken at 5-ps intervals. To include only the first hydration shell in the density calculation, the water molecules located within a distance of 3.5 Å and ions that are less than 4 Å from any of the DNA atoms were used to construct the water and ion densities. The 100 sets of individual structure factors for DNA and water coordinates were calculated after doing rigid body alignment with the starting coordinates, using unit cell parameters $a = 80$ Å, $b = 60$ Å, $c = 60$ Å, and $\alpha = \beta = \gamma = 90°$ at 1.5-Å resolution. The complex average of all structure factors was calculated and the amplitudes were treated as the experimental amplitudes. The average DNA coordinates were refined against the complex average structure factors using the simulated annealing protocol followed by positional and *B*-factor refinements. The *R*-factors for the working data set (R_{work}) and test set (R_{free}) were 26 and 27% respectively for the snapshots taken from a 1.5 to 2 ns interval, whereas for the 6.5–7 ns interval, the R_{work} and R_{free} were 18.3 and 19.1% respectively. The electron density for the water molecules and ions was calculated from the complex average structure factors by taking inverse Fourier transformation. All the pseudocrystallographic refinements were carried out using the CNS program (Brunger et al., 1998). The FRODO program (Jones, 1978) was used to display the calculated pseudoelectron densities. The calculated pseudoelectron densities were plotted against the refined average DNA structure.

RESULTS AND DISCUSSIONS

General characteristics

The MD trajectory of the 7-ns dynamics was quite stable and the duplex nature of the DNA molecule was retained throughout the simulation, even during the high temperature MD at 400 K (2–3 ns). The mean rmsd of the structures stored in that period with respect to the starting MD structure is 2.9 ± 0.45 Å. Two MD average structures were calculated for the snapshots stored between 1 and 2 ns and 6 and 7 ns to study the evolution of the DNA structure. The mean rmsd values for all the atoms with respect to the corresponding MD average structures are 1.2 Å ± 0.25 and 1.2 Å ± 0.23 for the above two ranges, whereas the rmsd between the heavy atoms of the two MD average structures is 0.78 Å. The low rmsd value between the two structures suggests that the DNA molecule had already reached an equilibrium structure during the first 1 ns of simulation. The rmsd plots for all atoms, as well as backbone and base atoms alone, for the 6–7 ns time period are shown in Fig. 1, and most of the subsequent analyses were carried out using the structures saved during 6–7 ns. The values of basepair propeller twist

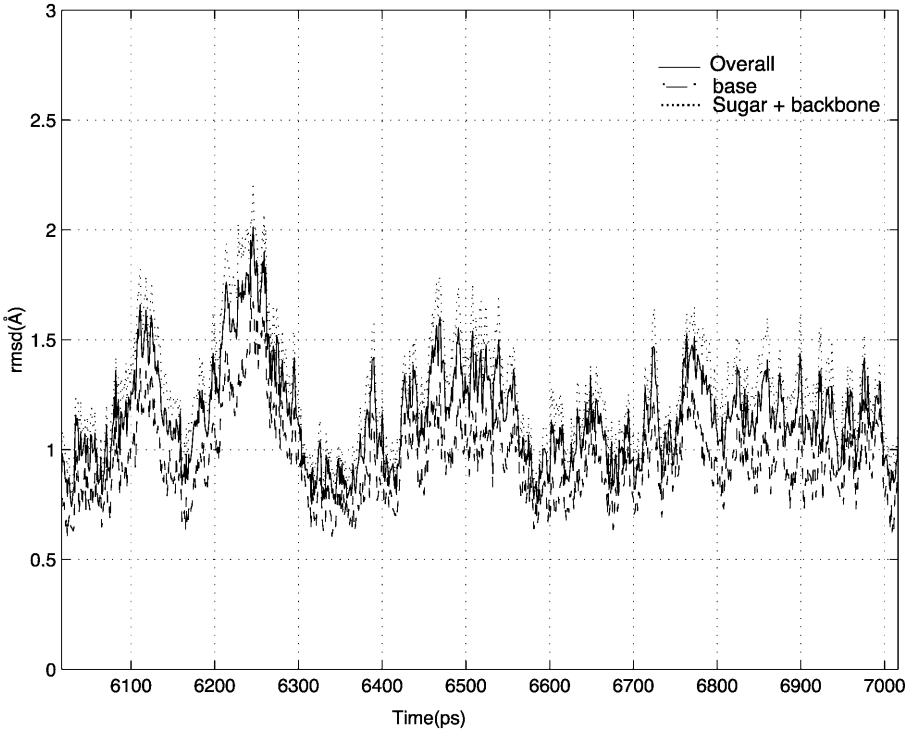

FIGURE 1 Trajectory plot for the 6–7-ns range showing the root mean square deviation for all atoms, base, and backbone atoms alone with respect to the MD average structure.

and the three important dinucleotide parameters (slide, roll, and twist) are given in Tables 1 and 2 and are compared with those observed in the crystal structure of the free form of A_3T_3 (pdb 1d65) as well as the average values of drug-bound complexes (pdb 102d, pdb 121d, pdb 1d63, pdb 263d, pdb 264d, pdb 296d, and pdb 2dnd). Some of the characteristic features of A-tract sequences like high propeller twist and small negative slide are well reproduced during the MD simulation and are comparable with the crystal structure values. The mean values of parameters for some steps (indicated by *) should be treated with caution, as they show a conformational transition from BI to the BII state (wherein ε and ξ take up the gauche$^-$ and *trans* conformation) for some period of time. The parameters for the terminal region show larger deviations due to the end effects in the MD simulations, although the fluctuations of parameters for the middle A-tract are generally within the ranges observed for free as well as bound form of the oligomer.

TABLE 1 The mean and standard deviations (in parentheses) of propeller twist for all the steps in the 6.5–7-ns range and their comparison with the crystal structure values of native and drug-bound forms

BP	Mean (6.5–7 ns)	A_3T_3	Mean of A_3T_3 + drugs
CG	−12.86 (12.51)	−17.83	−6.95 (6.9)
GC	−7.47 (9.20)	−12.55	−14.42 (4.98)
CG	−2.81 (7.68)	−6.8	−8.31 (4.43)
AT	−6.67 (7.51)	−11.69	−10.65 (5.02)
AT	−19.29 (6.73)	−19.64	−17.44 (3.38)
AT	−21.70 (7.55)	−20.29	−23.03 (3.52)
TA	−19.16 (6.54)	−15.14	−19.24 (3.66)
TA	−16.65 (7.19)	−18.21	−17.02 (0.72)
TA	−8.40 (6.87)	−14.64	−14.8 (4.64)
GC	−5.44 (8.73)	0.26	−4.63 (7.66)
CG	−10.49 (7.16)	−17.8	−20.79 (5.28)
GC	−21.99 (10.60)	13.31	0.87 (9.73)

Hydration

The results of fiber diffraction studies, as well as single crystal x-ray diffraction analyses have shown that the nucleic acid structure, stability, and recognition are greatly affected by hydration and it also plays a crucial role in triggering structural transitions between different duplex forms. The existence of a rich hydration network in the DNA minor groove (Neidle et al., 1980; Kopka et al., 1983; Berman, 1991, 1994), particularly, the ''spine'' that spans the entire AT-rich region (Brown et al., 1992; Kopka et al., 1983) was revealed from the crystal structure analysis of the Dickerson dodecamer. Later, premelting study (Chen and Prohofsky, 1992) on poly(dA).poly(dT) showed that this spine of hydration plays a significant role in enhancing the thermal stability of the basepairs to which they are attached. These hydration patterns are indeed of great importance because of their underlying relation to sequence dependent variations.

In our study, the average electron densities were generated for the water molecules located within 3.5 Å from any of the DNA atoms, as described in the Methods section. The electron density maps were calculated for each of the time frames between 1.5 and 2 ns (before heating), 3.5 and 4 ns, 4.5 and 5 ns, 5.5 and 6 ns, and 6.5 and 7 ns. The average

TABLE 2 The mean and standard deviation (in parentheses) of slide, roll, and twist for all the steps in the 6.5–7-ns range and their comparison with the crystal structure values of the native oligomer and its complexes with drugs

BP	MD	Slide A_3T_3	A_3T_3 + drugs	MD	Roll A_3T_3	A_3T_3 + drugs	MD	Twist A_3T_3	A_3T_3 + drugs
CG	−0.13 (0.54)	0.42	0.32 (0.18)	9.16 (6.31)	4.99	3.32 (1.52)	29.65 (8.98)	36.25	37.98 (2.76)
GC	0.37 (0.46)	0.54	0.34 (0.13)	−4.26 (5.13)	−5.82	−2.74 (1.7)	40.59* (5.00)	40.32	38.8 (0.48)
CA	−0.51 (0.36)	0.7	0.69 (0.2)	10.72 (4.30)	5.27	7.06 (2.47)	17.20 (4.08)	27	27.74 (1.46)
AA	−0.03 (0.35)	0.02	0.05 (0.1)	1.09 (6.3)	1.81	1.67 (1.21)	37.69* (5.65)	36.34	35.13 (1.74)
AA	−0.50 (0.40)	−0.03	−0.28 (0.15)	3.39 (4.51)	6.38	2.74 (3.86)	36.12* (3.76)	38.66	40.05 (2.4)
AT	−0.81 (0.30)	−0.63	−0.61 (0.11)	0.14 (4.40)	1.75	1.34 (1.69)	34.04 (2.62)	29.73	31.23 (1.38)
TT	−0.59 (0.40)	−0.05	−0.15 (0.22)	2.68 (5.19)	0.79	1.38 (2.47)	36.58 (3.66)	37.47	37.04 (1.31)
TT	−0.44 (0.54)	0.08	0.13 (0.14)	1.98 (4.75)	−2.78	−0.39 (3.39)	34.49* (5.97)	39.09	38.5 (1.47)
TG	−0.45 (0.44)	0.99	0.2 (0.2)	12.48 (5.36)	0.9	−0.61 (3.38)	20.95 (4.99)	30.65	32.23 (1.25)
GC	0.01 (0.36)	0.82	0.58 (0.3)	−2.71 (4.9)	−8.78	−9.56 (2.31)	38.96* (3.40)	40.35	38.07 (1.78)
CG	1.33 (0.62)	0.67	0.66 (0.22)	14.87 (5.35)	−7.24	0.1 (5.29)	31.29 (4.16)	38.15	38.78 (1.05)

*G2C3, G10C11, A5A6 steps, and A4A5 in both strands show transition to BII conformation for some period of time.

electron density versus refined average simulated structure for the two ranges (1.5–2 ns and 6.5–7 ns) are shown in Fig. 2, *a* and *b*. The calculated electron density map clearly shows that a sequence dependent hydration pattern starts to form in the minor groove during the initial stage itself (Fig. 2 *a*). However a striking improvement in the water densities was seen after the 1 ns equilibration (2–3 ns) at 400 K, which obviously facilitated the rearrangement of water molecules. This is also reflected in the reduction of the crystallographic *R*-factor from 26 to 21% for the two structures calculated in the 1.5–2-ns and 3.5–4-ns ranges. Interestingly, the characteristic sequence dependent hydration pattern that was formed in the 3.5–4-ns range is retained in the extended MD (6–7 ns), though the *R*-factor reduced to 18%, indicating further immobilization of the water molecules. The solvent densities, which are halfway between the basepair planes, bridge two basepairs through favorable hydrogen bonds. The density map for the 6.5–7-ns (Fig. 2 *b*) range shows a fairly high density of water near the DNA backbone, though the water molecules are expected to be mobile in these regions.

The peaks that are above 5.5 σ in the calculated electron density map during the last 500-ps (6.5–7 ns) range are identified as sites for stable or structurally important water molecules and the refined average simulated structure with fitted water molecules is shown in Fig. 3. The minor groove and major groove hydration patterns are shown schematically in Fig. 4, *a* and *b*, respectively. The rich network of water molecules in the minor groove (Fig. 4 *a*) shows a clear sequence signature. A ribbon is formed near the 5′ and 3′ GC rich ends of the duplex, bridging inter- and intrastrand bases via O2 of C, N2, and N3 atoms of G. This extends as a spine of water molecules, into the A_3T_3 region, which bridges the N3 of A and O2 of T in an interstrand manner. There is an extensive involvement of sugar O4′ atoms also in the minor groove hydration pattern. This type of sequence dependent DNA hydration pattern is also reported to be present in the high resolution (1.1 Å) crystal structure of A_2T_2 structure (Tereshko et al., 1999b). Here a complex pattern of fused water hexagons was seen in the minor groove, but the interaction of DNA with waters forming the inner hexagon corners is identical to the original spine. Interestingly, the sequence dependent hydration features are more pronounced in our MD simulation than in the medium resolution (2.2 Å) crystal structure of this A_3T_3 sequence (Edwards et al., 1992) where, in contrast to the spine, an extended ribbon of water molecules is seen in the minor groove. The hydration cones formed by three water molecules around the anionic oxygen atom of some phosphate groups are also easily recognizable (see Fig. 3). This is in agreement with the earlier reported crystal structure analysis of hydration of phosphate groups in double helical DNA structure (Schneider et al., 1998) and results from MD studies (Duan et al., 1997; Beveridge et al., 1990).

Several bound water molecules are also observed in the major groove (Fig. 2 *b*), but no specific pattern is observed. An extensive network of water bridges is formed between N4-C, O6-G, N6 or N7-A, and O4-T atoms in the major groove, especially in the central AT rich regions. Such a pattern has not been reported for the crystal structure of A_3T_3 oligomer, but our observation of the more extensive water interaction pattern is in good agreement with the high resolution A_2T_2 crystal structure (Tereshko et al., 1999a).

Groove width and ion effect

Although the intrinsic sequence dependent variation and narrowing of the minor groove in the A-tract region is generally accepted, an alternative view has been presented recently (Woods et al., 2000; McFail-Isom et al., 1999). This suggests that the sequence dependent localization of cations and water molecules plays a key role in determining the groove structure. Since the sodium counterions in nucleic acid crystals have escaped detection with very few exceptions (Seeman et al., 1976) the cause for groove narrowing is still a matter of debate. The recent high resolution crystal structure (Tereshko et al., 1999a) of A_2T_2 duplex also did not find any evidence for the presence of monovalent sodium ions in the minor groove.

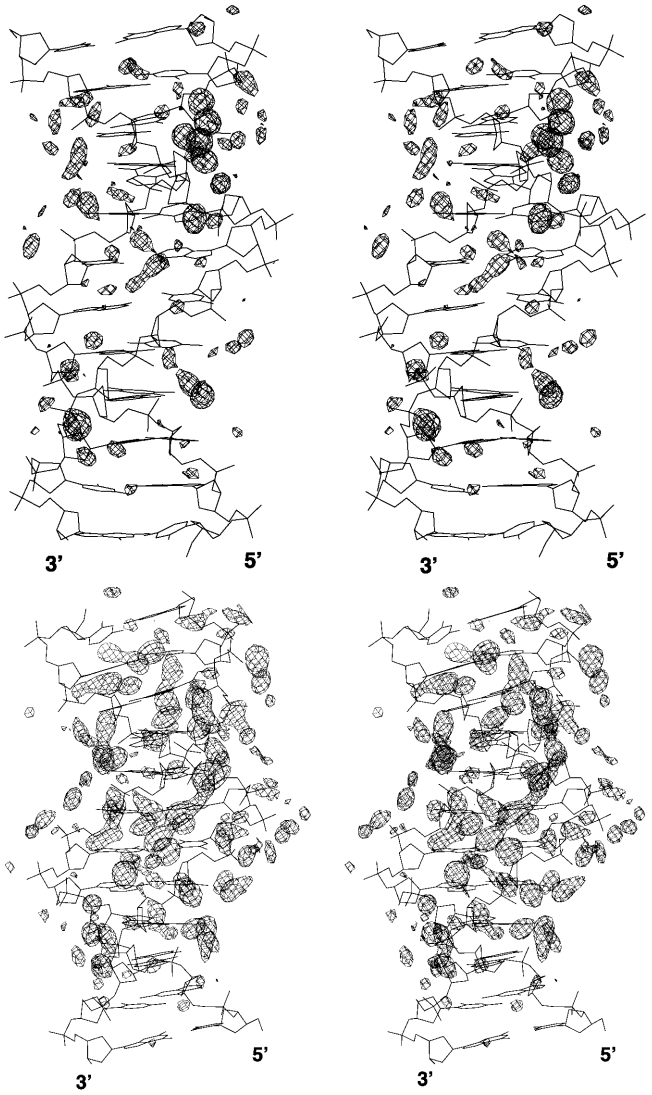

FIGURE 2 Stereo diagrams showing the pseudocrystallographically refined structure versus average solvent density. (*a*) The refined average DNA coordinates were obtained from the structures stored during the range 1.5–2 ns. (*b*) For the structures stored during 6.5–7 ns of MD simulation. For the calculation of electron density map, the water molecules within 3.5 Å were considered. Solvent density displayed here corresponds to 5-σ contours. Here the minor groove spine of hydration pattern is clearly seen from the densities. Electron density corresponding to the cone of hydration is also seen near some backbone phosphate groups.

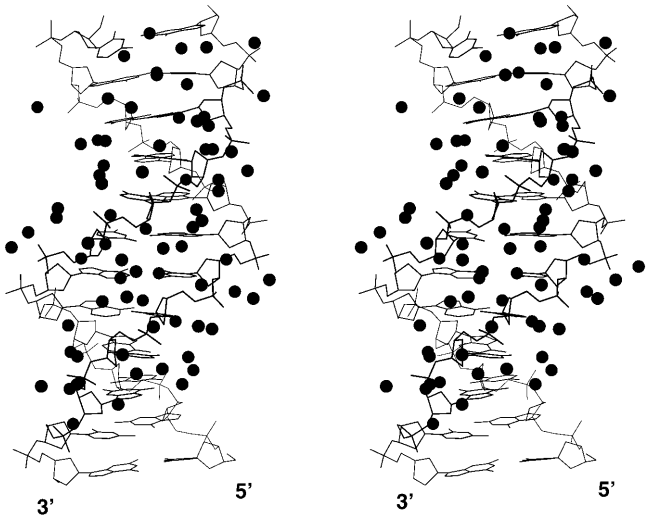

FIGURE 3 Represented here is the crystallographically refined average DNA structure against the water molecules fitted for the contours obtained with a 5.5-σ cutoff. This higher cutoff is chosen to get water densities corresponding to more stable waters. The average DNA structure was calculated for the snapshots taken between 6.5 and 7 ns. Here the spine of hydration in the minor groove as well as the cone of hydration around the backbone P atoms is clearly seen. The actual hydrogen bond patterns are shown in Fig 4.

During the course of our MD simulation the minor groove width undergoes considerable fluctuations from the starting fiber value of 11.7 Å. As a measure of groove width, the minimal interstrand phosphorous distances were calculated using our in-house program and the distances for 1.5–2 ns as well as for 6.5–7 ns are tabulated in Table 3. The minor groove width in the central A-tract region is smaller than that of terminal regions, in both the ranges. The groove width trend along the sequence is comparable with that seen in the crystal structure of the free oligomer, as well as in its complex forms (Fig. 5), except for the distance involving the phosphate P11 of strand 1 and P7 of strand 2. The unusually large deviation in the interstrand P. . .P distance spanning the dinucleotide steps T8T9 and T9G10 may be due to a high positive roll angle at the T9G10 step, accompanied by a BII conformation in the neighboring step, which is observed during the MD simulation. In general, the variation in the groove width toward the 3′ end among the drug-bound complexes is attributed to the effect of changes in the local parameters to accommodate a wide variety of ligands.

To address the issue of groove narrowing possibly being due to localized counterions, we monitored ions located within a 4-Å distance from any of the DNA atoms. Only ions showing more than 50% occupancy in any location are considered as structurally important, since they can be part of the primary hydration shell. Out of 22 counterions, only one ion is found to have more than 50% occupancy in the 6–7-ns range and this is found to occur near the backbone. The minor groove of A-tracts is found to be completely devoid of ions. Despite the absence of ions in the minor groove, the groove width in the A-tract region is smaller than the starting fiber value of 11.7 Å from an early period of dynamics (13 ps) and this feature is maintained throughout the dynamics. The calculated ion density map (Fig. 6) also confirms the presence of ions near the backbone, rather than in the vicinity of the A-tract region. The ion density map has also been calculated for four different ranges of MD time scale: 3.5–4 ns, 4.5–5 ns, 5.5–6 ns, and 6.5–7 ns. During the first range of 3.5–4 ns, strong ion densities were seen at the start (A4) as well as near the end (G10) of the A-tracts. During the 4.5–5-ns interval, more ion densities were seen around the backbone than in the previously located floor of the minor

groove. But in the last two ranges (5.5–6 ns, 6.5–7 ns) strong ion densities were seen only around the backbone and there was absolutely no trace of ion density in the minor groove. Thus from the MD study it can be concluded that monovalent cations (Na^+ ions) can be part of the primary hydration shell, but the low percentage of occupancy implies that it as a rare event and also that groove bound ions do not play a major role in groove narrowing. This fact is also confirmed by ^{23}Na magnetic relaxation dispersion measurement experiments (Denisov and Halle, 2000) as well as by recent MD study of A-tract containing sequences (McConnell and Beveridge, 2000). Therefore, the main cause for the groove narrowing can be attributed to the intrinsic sequence dependent features such as high propeller twist and negative slide in the A-tract region. The mean and standard deviations of propeller twist, roll, and slide values at each step are listed in Tables 1 and 2.

Cross-strand hydrogen bonds

One of the sequence dependent signatures observed in DNA oligomer crystal structures is the occurrence of favorable cross-strand interactions or bifurcated hydrogen bonds. The possibility of a bifurcated hydrogen bond across the major groove between the N6–H atom of adenine on one strand of the DNA duplex and the O4 atom of a thymine, located on the 3′ side of a W.C pair, on the other strand, has been proposed on the basis of crystal structure evidence (Nelson et al., 1987). This interaction is facilitated mainly by the relatively large propeller twist for the A.T basepairs constituting the AA step, and was suggested as contributing to the stability and rigidity of the structure. Subsequently, other potential cross-strand interactions like N–H. . .N, C–H. . .N, and C–H. . .O in major groove as well as in minor groove were reported for different sequences (Nelson et al., 1987; Shatzky-Schwartz et al., 1997; Luisi et al., 1998; Ghosh and Bansal, 1999a,b). All possible cross-strand interactions in the major as well as minor grooves in our sequence are shown schematically in Fig. 7.

MD snapshots were checked for all possible cross-strand C–H. . .N, N–H. . .N, and N–H. . .O hydrogen bonds in the minor and major grooves. The frequency of H. . .O distances for N6H. . .O4 cross-strand hydrogen bond is centered around 3.2–3.4 Å. The percentage occurrence of an

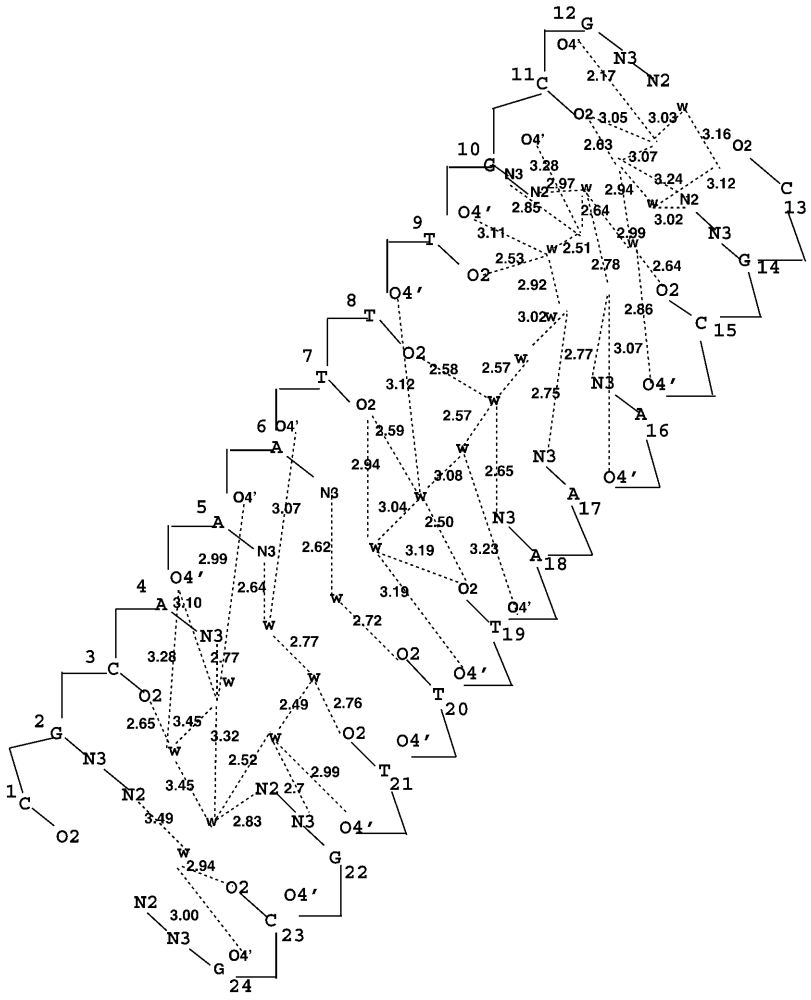

FIGURE 4 (*a* and *b*) Schematic representations of minor and major groove hydration patterns in the 6.5–7-ns period are shown here with the H. . .O distances <3.5 Å being indicated by dotted lines.

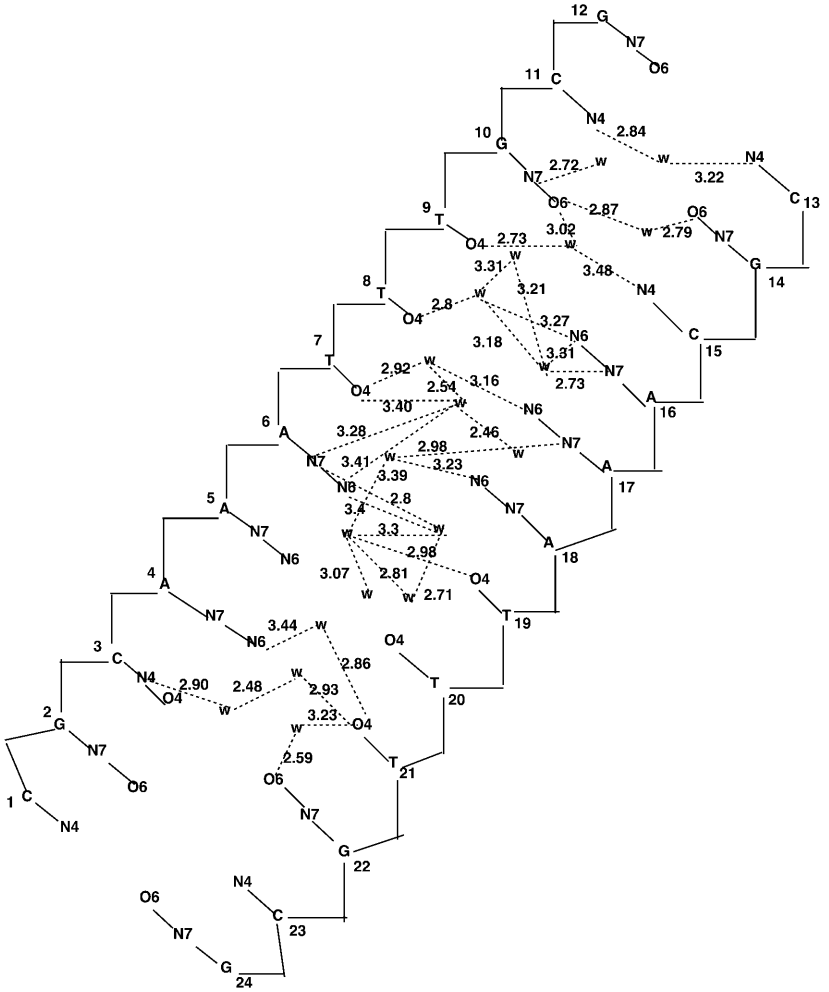

FIGURE 4 Continued.

N–H. . .O type of hydrogen bond (defined by H. . .O distances <2.8 Å) in the major groove, ranges between 1.5 and 11% indicating the rare occurrence of this type of interaction. This observation is in agreement with the results of an earlier reported crystallographic database analysis (Ghosh and Bansal, 1999b) and the MD studies on A-tracts (Sherer et al., 1999; McConnell and Beveridge, 2001). In addition, very often even when the N. . .O and N. . .N distances are shorter than the equilibrium distances (i.e., <3.5 Å), the H. . .O, H. . .N distances are greater than 2.8 Å, indicating the poor geometry of these hydrogen bonds.

TABLE 3 The mean and standard deviations (in parentheses) of minimal interstrand P. . .P distances for the structures stored during the 1.5–2-ns and 6.5–7-ns ranges

Mean (1.5–2 ns)	Mean (6.5–7 ns)	A_3T_3	Mean of A_3T_3 + drugs
10.24 (1.59)	13.55 (1.11)	13.81	13.93 (0.24)
11.48 (1.29)	12.16 (1.17)	12.62	12.51 (0.19)
10.17 (1.11)	10.70 (0.95)	10.74	10.82 (0.29)
10.19 (0.83)	9.98 (0.64)	10.36	10.11 (0.38)
10.10 (0.76)	10.03 (0.90)	10.33	10.29 (0.21)
10.70 (0.89)	11.03 (0.89)	10.52	10.18 (0.34)
12.75 (0.73)	13.67 (0.76)	11.51	11.85 (0.46)
12.43 (0.69)	12.52 (0.86)	11.14	10.83 (0.34)

The P. . .P interstrand distances in the free form of A_3T_3 crystal structure as well as the average and standard deviations in the drug-bound complexes are also shown for comparison.

C–H. . .O hydrogen bonds in the minor groove

Yet another type of cross-strand hydrogen bond is possible in the minor groove of A-tracts, viz. the rarely discussed C–H. . .O interaction (also shown in Fig. 7). Analysis of B-DNA type oligomeric crystal structures as well as protein bound DNA fragments showed that a significant number of C–H. . .O hydrogen bonds are present in the minor groove (Ghosh and Bansal, 1999a,b). The ensembles of MD structures were therefore examined for all possible cross-strand C–H. . .O hydrogen bonds. The frequency of the possible cross-strand interactions between C2H2 of adenine and O2 of thymine, as characterized by the H2. . .O2 distances for the 1–2-ns and 6–7-ns ranges are shown in Fig. 8. The C–H. . .O type of hydrogen bond is found to exist between cross-strand basepairs 5A. . .9T, 6A. . .8T, 8T. . .6A, and 9T. . .5A and the percentage of occurrence of H. . .O

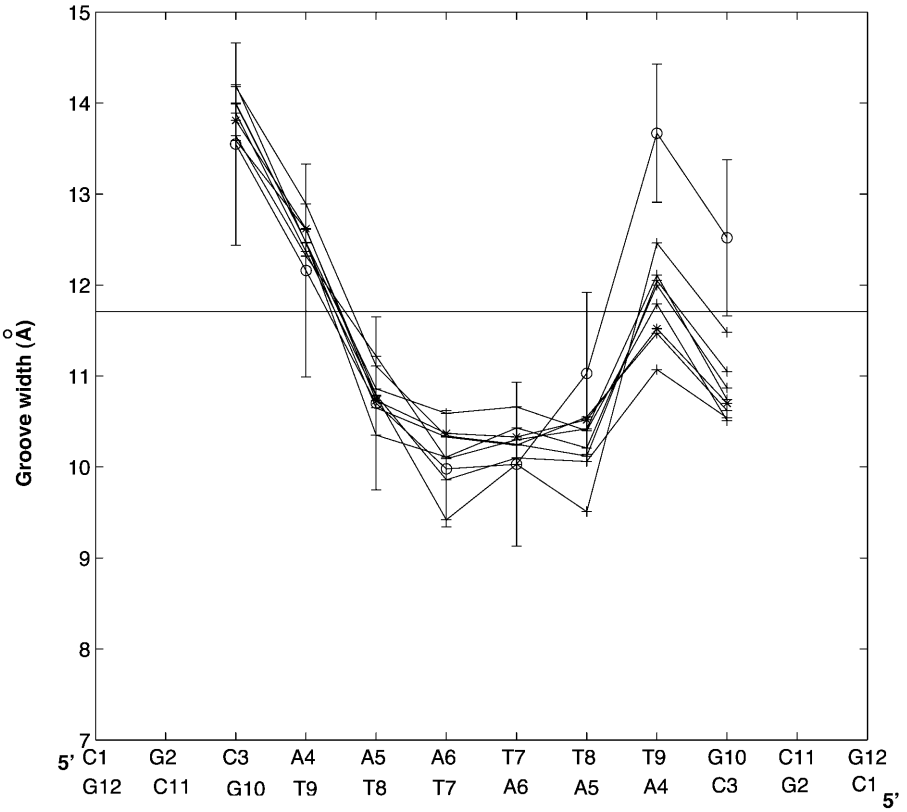

FIGURE 5 Minor groove width plotted along the sequence for MD average values for the structures stored in the 6.5–7-ns range and the crystal structures of free and bound forms. Open circles represent the points from MD average structure, with error bars varying between $\pm$ 1 σ, "*" symbol represents the points from crystal structure (pdb 1d65), and "+" symbol represents the points from drug-DNA complexes (pdb 102d, pdb 121d, pdb 1d63, pdb 263d, pdb 264d, pdb 296d, pdb 2dnd, and pdb 403d). The data points have been aligned so as to indicate the P...P distance across the dinucleotide steps viz. the first point corresponds to the interstrand distance between P5 in strand 1 and P12 of strand 2 and spans the dinucleotide steps G2C3 and C3A4. The horizontal line indicates the uniform interstrand P...P distance (11.7 Å) for the starting fiber model.

distances less than 2.8 Å in the above cases are 55.1%, 68.1%, 69.5%, and 60.5% during the 6–7-ns range, as compared to 42.1%, 58.8%, 57.7%, and 75.5% during the 1–2-ns range. Thus, in addition to the cross-strand C–H...O hydrogen bonds seen in the free form of A_3T_3 crystal structure (5A...9T and 9T...5A), our MD study shows the possibility of potential cross-strand C–H...O hydrogen bonds in other AA.TT steps (6A...8T, 8T...6A). These dinucleotide steps are also found to have favorable C–H...O hydrogen bonds in many of the drug-bound complexes (pdb 2dnd, pdb 296d, pdb 264d, pdb 1d63, and pdb 102d) with the A_3T_3 sequence. The frequent occurrence of C–H...O hydrogen bonds in the A_3T_3 sequence indicates that it is quite a ubiquitous feature of A-tracts.

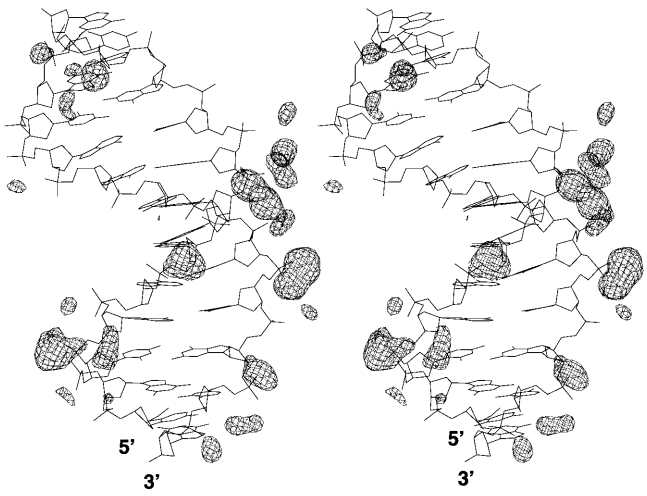

FIGURE 6 Stereo diagram shows the refined average structure versus ion density calculated for the structures stored in the 6.5–7-ns range. The ion density is calculated for the ions, which are within 4 Å to any of the DNA atoms. Ion densities represented here correspond to 8-σ contours and hence represent highly localized ion sites.

Database analysis of crystal structures, of free as well as protein-bound form of A-tract DNA fragments, had shown that the occurrence of C–H...O type of interaction depends on characteristic local parameters such as smaller basepair opening angle and interbasepair slide, in addition to the well-noted high propeller twist in these regions (Ghosh and Bansal, 1999b). To identify the basis of potentially favorable C–H...O hydrogen bonds from MD trajectories, the correlation coefficients were calculated for H...O distances and various local step (shift, slide, rise, tilt, roll, and twist) and intrabasepair parameters (propeller, buckle, and opening angle). There is a significant correlation only between H...O distances of cross-strand basepair 5A...9T and the corresponding roll, twist, shift, and slide values, with correlation coefficient values of 0.68, −0.47, 0.51, and 0.45. This could be due to BII type of conformation in A4A5 step of strand 1. No significant correlation is found between H...O distances of other cross-strand basepairs and these parameters. Thus interestingly, short C–H...O distance appears to be the cumulative effect of various parameters. For example at

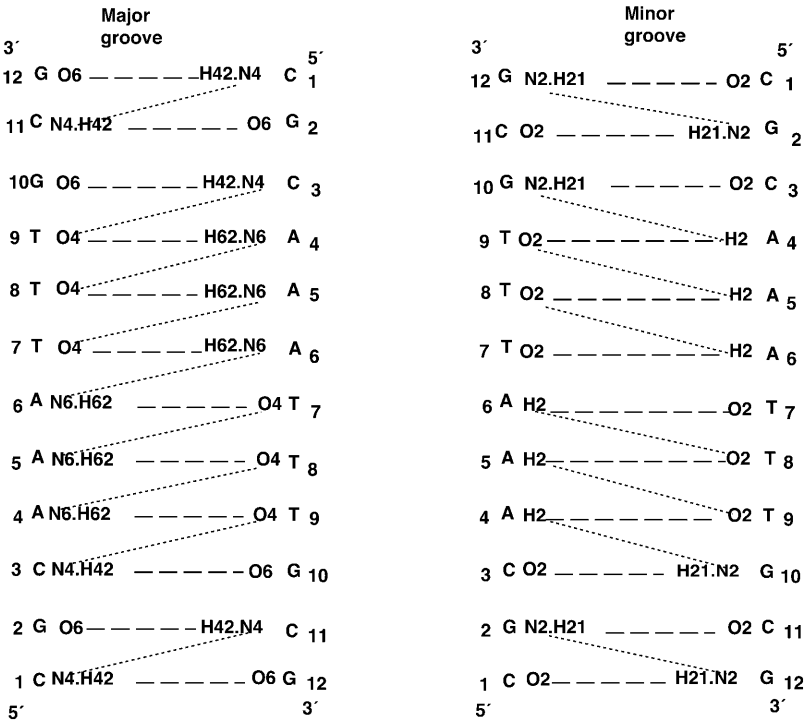

FIGURE 7 Schematic diagram showing cross-strand major and minor groove interactions corresponding to potential cross-strand hydrogen bonds.

3207 ps when the H. . .O distance is 2.47 Å, the corresponding slide value is 0.16 Å and roll has a high negative value of −9.33 Å. Hence even when the slide is positive, negative roll enhances C–H. . .O hydrogen bond in the minor groove. Thus there appears to be a greater preference for C–H. . .O type of cross-strand hydrogen bonds in the minor groove, rather than the N–H. . .O type of cross-strand hydrogen bonds in the major groove.

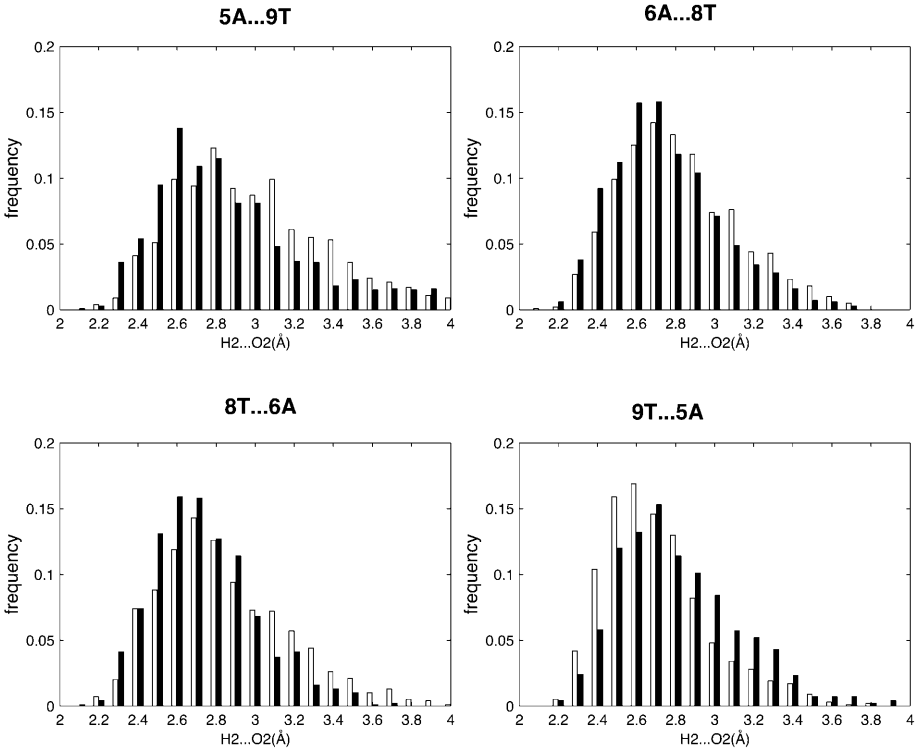

FIGURE 8 Plot showing the frequency of occurrence of cross-strand H. . .O distances in the minor groove taken from MD snapshots of 1–2 ns (*open bars*) and 6–7 ns (*filled bars*).

Comparison of MD simulated structures with free and drug-bound crystal structures

Drug-DNA interaction is highly base sequence specific, mainly because of the differences in the spatial arrangements of DNA donor/acceptor atoms in the minor groove. Many drugs like netropsin, berenil, pentamidine, Trisbenzimidazole, Hoechst- 33258, and distamycin bind preferentially to the AT region of the minor groove of the A_3T_3 structure (Brown et al., 1992; Tabernero et al., 1993; Cristina Vega et al., 1994; Spink et al., 1994; Clark et al., 1996a,b; Nunn and Neidle, 1995; Coll et al., 1987). Our MD study on the structure of A_3T_3 in the absence of any bound ligands provides some insights into the extent of flexibility of this sequence to accommodate a variety of ligands in the AT rich minor groove. The rmsd between all the heavy atoms in the crystal structure of this A_3T_3 sequence (Edwards et al., 1992) and the MD average structure for the ranges between 1 and 2 ns and 6 and 7 ns is 1.80 and 1.68 Å, whereas the rmsd for the middle A_3T_3 region is much smaller at 1.06 and 0.55 Å, respectively, again confirming that the characteristic structure of the A-tract region is formed quite early in the dynamics. To check whether our dynamics has sampled conformations of drug-bound complexes, the rmsd between each of the drug-bound complex structure and the MD average structure for A_3T_3 region alone was calculated and it ranges between 0.48 and 0.65 Å. A comparison of the above two rmsds, one with respect to free form and the other with drug-bound complexes, shows that the MD average structure with its well-defined hydration patterns is very similar to the drug-bound complexes as well as to the free form of the A_3T_3 crystal structure. As an example, the superposition of the A_3T_3 region of distamycin complex on the MD average structure is shown in Fig. 9. All the basepair parameters calculated from MD structures (Tables 2 and 3) also fluctuate within the range observed in free and drug-bound forms, except at the termini. This indicates that the ranges of deformability of this sequence sampled by the MD study are essential for the binding of a large variety of ligands, which recognize this sequence.

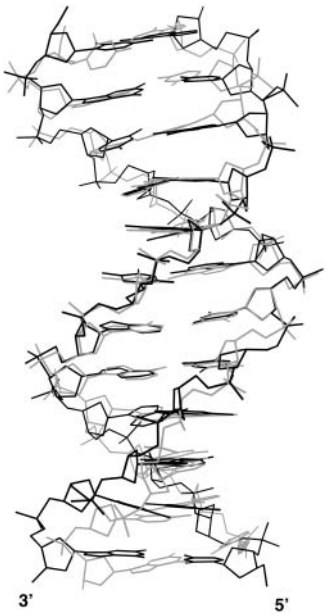

FIGURE 9 The superposition of the A_3T_3 region of the MD average structure calculated in the 6–7-ns range (*gray*) and the A_3T_3 + distamycin (*black*) complex are shown and the rmsd between the two structures in the region is 0.57 Å.

CONCLUSION

On the basis of our MD study it can be concluded that the duplex formed by A_3T_3 sequence has characteristic sequence dependent features and it is flexible enough to accommodate a wide variety of drug molecules in the minor groove. The characteristic minor groove spine of hydration in the AT region and the ribbon of hydration in the GC rich region is surprisingly well pronounced in our dynamic DNA model. In fact the hydration pattern is more well defined than that reported for the medium resolution crystal structure, where no clear-cut hydration pattern was observed in the GC regions. Similarly, the prominent major groove hydration observed in the central AT region from our MD study is not seen in the crystal structure of this sequence but has been reported in other related sequences. MD results suggest that the effect of monovalent Na^+ counterions, as well as specific hydration pattern, on the groove width is insignificant and the characteristic narrow minor groove in the A-tract regions can be primarily attributed to high propeller twist and negative slide at these dinucleotide steps. Cross-strand C–H. . .O hydrogen bonds are seen between 5A. . .9T, 6A. . .8T, 8T. . . 6A, and 9T. . .5A during MD, similar to those found to occur in the crystal structures of free and drug-bound forms of this and other A-tract sequences. It is also interesting to note that this characteristic C–H. . .O interaction in the minor groove is preferred over the N–H. . .O type of cross-strand hydrogen bonds in the major groove of A-tract sequences, and possibly helps to stabilize the oligo(A) tract structure with its narrow minor groove. The characteristic cross-strand C2–H2. . .O2 hydrogen bonds in the minor groove of A-tract sequences are well reproduced in the study and are found to occur even before the narrowing of the minor groove and formation of the well-defined spine of hydration. Hence the ubiquitous nature of C2–H2. . .O2 cross-strand hydrogen bonds is confirmed as an intrinsic feature of A-tract DNA structure.

The authors are grateful to Supercomputer Education and Research Centre, Indian Institute of Science for computational facilities. The authors acknowledge A.A. Jeyaprakash for many useful discussions on crystallographic techniques.

The work is supported by a Council for Scientific and Industrial Research grant, India.

REFERENCES

Bansal, M., D. Bhattacharya, and B. Ravi. 1995. NUPARM and NUCGEN: software for analysis and generation of sequence dependent nucleic acid structures. *Comput. Appl. Biosci.* 11:281–287.

Berman, H. M. 1991. Hydration of DNA. *Curr. Opin. Struct. Biol.* 1:423–427.

Berman, H. M. 1994. Hydration of DNA: take 2. *Curr. Opin. Struct. Biol.* 4:345–350.

Beveridge, D. L., P. Subramanian, B. Jeyaram, S. Swaminathan, and G. Ravishanker. 1990. Molecular simulation studies on the d(CGCG-AATTCGCG) duplex: hydration, ion atmosphere, structure and dynamics. *J. Biomol. Struct. Dyn.* 3:79–112.

Bhattacharya, D., and M. Bansal. 1989. A self-consistent formulation for analysis and generation of non-uniform DNA structures. *J. Biomol. Struct. Dyn.* 6:635–653.

Bonvin, M. J. J. A. 2000. Localisation and dynamics of sodium counterions around DNA in solution from molecular dynamics simulation. *Eur. Biophys. J.* 29:57–60.

Brown, D. G., M. R. Sanderson, E. Garman, and S. Neidle. 1992. Crystal structure of a Berenil-d(CGCAAATTGCG) complex an example of drug-DNA recognition based on sequence-dependent structural features. *J. Mol. Biol.* 226:481–490.

Brown, D. G., M. R. Sanderson, J. V. Skelly, T. C. Jenkins, T. Brown, E. Garman, D. I. Stuart, and S. Neidle. 1990. Crystal structure of a Berenil-dodecanucleotide complex: the role of water in sequence-specific ligand binding. *EMBO J.* 9:1329–1334.

Brunger, A. T., P. D. Adams, G. M. Clore, W. L. Delano, P. Gros, R. W. Grosse-Kunstleve, J. S. Jiang, J. Kuszeroski, M. Nilges, N. S. Pannu, R. J. Read, T. Simonson, and G. L. Warren. 1998. Crystallography & NMR system: a new software suite for macromolecular structure determination. *Acta Crystallogr.* 54:905–921.

Burkhoff, A. M., and T. D. Tullius. 1987. The unusual conformation adopted by the adenine tracts in kinetoplast DNA. *Cell.* 48:935–943.

Chen, Y. Z., and E. W. Prohofsky. 1992. The role of a minor groove spine of hydration in stabilizing poly(dA). poly(dT) against fluctuational interbase H-bond disruption in the premelting temperature regime. *Nucleic Acids Res.* 20:415–419.

Chiu, T. K., and R. E. Dickerson. 2000. 1 Å crystal structures of B-DNA reveal sequence-specific binding and groove specific bending of DNA by magnesium and calcium. *J. Mol. Biol.* 301:915–945.

Chiu, T. K., M. Kaczor-Greskowiak, and R. E. Dickerson. 1999. Absence of minor groove monovalent cations in the crosslinked dodecamer C-G-C-A-A-T-T-C-G-C-G. *J. Mol. Biol.* 292:598–608.

Clark, G. R., E. J. Gray, and S. Neidle. 1996a. Isohelicity and phasing in drug-DNA sequence recognition: crystal structure of a Tris (benzimidazole)-oligonucleotide complex. *Biochemistry.* 35:13745–13752.

Clark, G. R., C. J. Squire, E. J. Gray, W. Leupin, and S. Neidle. 1996b. Designer DNA-binding drugs: the crystal structure of a meta-hydroxy analogue of Hoechst 33258 bound to d(CGCGAATTCGCG)2. *Nucleic Acids Res.* 24:4882–4889.

Coll, M., C. A. Frederick, A. H. Wang, and A. Rich. 1987. A bifurcated hydrogen-bonded conformation in the d(A.T) basepairs of the DNA dodecamer d(CGCAAATTTGCG) and its complex with distamycin. *Proc. Natl. Acad. Sci. USA.* 84:8385–8389.

Constanz, G., E. Di Mauro, G. Salina, and R. Negri. 1990. Attraction, phasing and neighbour effects of histone octamers on curved DNA. *J. Mol. Biol.* 216:363–374.

Cornell, W. D., P. Cieplak, C. I. Bayly, I. R. Gould, K. M. Merz, Jr., D. M. Ferguson, D. C. Spellmeyer, T. Fox, J. W. Caldwell, and P. A. Kollman.1995. A second generation force field for the simulations of proteins, nucleic acids and organic molecules. *J. Am. Chem. Soc.* 117: 5179–5197.

Cristina Vega, M., I. Garcia Saez, J. Aymami, R. Eritja, G. A. Van der Marel, J. H. Van Boom, A. Rich, and M. Coll. 1994. Three-dimensional crystal structure of the A-tract DNA dodecamer d(CGCAAATTTGCG) complexed with the minor-groove-binding drug Hoechst 33258. *Eur. J. Biochem.* 222:721–726.

Darden, T., D. York, and L. Pedersen. 1993. Particle mesh Ewald—an N.logn method for Ewald sums in large systems. *J. Chem. Phys.* 98: 10089–10092.

Denisov, V. P., and B. Halle. 2000. Sequence-specific binding of counterions to B-DNA. *Proc. Natl. Acad. Sci. USA.* 97:629–633.

Drew, H. R., and R. E. Dickerson. 1981. Structure of a B-DNA dodecamer. III. Geometry of hydration. *J. Mol. Biol.* 151:535–556.

Duan, Y., P. Wilkosz, M. Crowley, and J. M. Rosenberg. 1997. Molecular dynamics simulation study of DNA dodecamer d(CGCGAATTCGCG) in solution: conformation and hydration. *J. Mol. Biol.* 272:553–572.

Edwards, K. J., D. G. Brown, N. Spink, J. V. Skelly, and S. Neidle. 1992. Molecular structure of B-DNA dodecamer d(CGCAAATTTGCG)$_2$. *J. Mol. Biol.* 226:1161–1173.

Edwards, K. J., T. C. Jenkins, and S. Neidle. 1992. Crystal structure of a pentamidine oligonucleotide complex: implications for DNA-binding properties. *Biochemistry.* 31:7104–7109.

El Hassan, M. A., and C. R. Calladine. 1998. Two distinct modes of protein-induced bending in DNA. *J. Mol. Biol.* 282:331–343 (Review.).

Feig, M., and M. B. Pettit. 1999. Sodium and chloride ions as part of the DNA solvation shell. *Biophys. J.* 77:1769–1781.

Ghosh, A., and M. Bansal. 1999a. Three-centre C-H. . .O hydrogen bonds in the DNA minor groove: analysis of oligonucleotide crystal structures. *Acta Crystallogr. D.* 55:2005–2012.

Ghosh, A., and M. Bansal. 1999b. C-H.O hydrogen bonds in minor groove of A-tracts in DNA double helices. *J. Mol. Biol.* 294:1149–1158.

Goodsell, D. S., H. L. Ng, M. L. Kopka, J. W. Lown, and R. E. Dickerson. 1995. Structure of a dicationic monoimidazole lexitropsin bound to DNA. *Biochemistry.* 34:16654–16661.

Hamelberg, D., L. McFaill-Isom, L. D. Williams, and W. D. Wilson. 2000. Flexible structure of DNA: ion dependence of minor-groove structure and dynamics. *J. Am. Chem. Soc.* 120:10513–10520.

Hamelberg, D., L. D. Williams, and W. D. Wilson. 2001. Influence of dynamic positions of cations on the structure of the DNA minor groove: sequence-dependent effects. *J. Am. Chem. Soc.* 123:7745–7755.

Howerton, S. B., C. C. Sines, D. Vanderveer, and L. D. Williams. 2001. Locating monovalent cations in the grooves of B-DNA. *Biochemistry.* 40:10023–10031.

Hud, N. V., and J. Feigon. 1997. Localisation of divalent metal ions in the minor groove of DNA A-tracts. *J. Am. Chem. Soc.* 119:5756–5757.

Hud, N. V., V. Sklenar, and J. Feigon. 1999. Localization of ammonium ions in the minor groove of DNA duplexes in solution and the origin of DNA A-tract bending. *J. Mol. Biol.* 286:651–660.

Jones, T. A. 1978. A graphics model building and refinement system for macromolecules. *J. Appl. Crystallogr.* 11:268–272.

Kopka, M. L., A. V. Fratini, H. R. Drew, and R. E. Dickerson. 1983. Ordered water structure around a B-DNA dodecamer—a quantitative study. *J. Mol. Biol.* 163:129–146.

Kopka, M. L., C. Yoon, D. Goodsell, P. Pjura, and R. E. Dickerson. 1985. Binding of an antitumor drug to DNA. Netropsin and C-G-C-G-A-A-T-T-BrC-G-C-G. *J. Mol. Biol.* 183:553–563.

Larsen, T., D. S. Goodsell, D. Cascio, K. Grzeskowiak, and R. E. Dickerson. 1989. The Structure of DAPI bound to DNA. *J. Biomol. Struct. Dyn.* 7:477–491.

Laughton, C. A., F. Tanious, C. M. Nunn, D. W. Boykin, W. D. Wilson, and S. Neidle. 1996. A crystallographic and spectroscopic study of the complex between d(CGCGAATTCGCG)2 and 2,5-bis(4-guanylphenyl)-furan, an analogue of berenil. Structural origins of enhanced DNA-binding affinity. *Biochemistry.* 35:5655–5661.

Liepinsh, E., G. Otting, and K. Wuthrich. 1992. NMR observation of individual molecules of hydration water bound to DNA duplexes: direct evidence for a spine of hydration water present in aqueous solution. *Nucleic Acids Res.* 20:6549–6553.

Luisi, B., M. Orozco, J. Sponer, F. J. Luque, and Z. Shakked. 1998. On the potential role of the amino nitrogen atom as a hydrogen bond acceptor in macromolecule. *J. Mol. Biol.* 279:1123–1136.

McConnell, K. J., and D. L. Beveridge. 2000. DNA structure: what's in charge? *J. Mol. Biol.* 304:803–820.

McConnell, K. J., and D. L. Beveridge. 2001. Molecular dynamics simulations of B′-DNA: sequence effects on A-tract-induced bending and flexibility. *J. Mol. Biol.* 314:23–40.

McFail-Isom, L., C. C. Sines, and L. D. Williams. 1999. DNA structure: cations in charge? *Curr. Opin. Struct. Biol.* 9:298–304.

Minasov, G., V. Tereshko, and M. Egli. 1999. Atomic-resolution crystal structures of B-DNA reveal specific influences of divalent metal ions on conformation and packing. *J. Mol. Biol.* 291:83–99.

Neidle, S., H. M. Berman, and H. S. Shieh. 1980. Highly structured water network in crystals of a deoxydi-nucleoside-drug complex. *Nature.* 288:129–133.

Nelson, H. C. M., J. T. Finch, B. F. Luisi, and A. Klug. 1987. The structure of an oligo(dA). oligo(dT) tract and its biological implications. *Nature.* 330:221–226.

Nunn, C. M., and S. Neidle. 1995. Sequence-dependent drug binding to the minor groove of DNA: crystal structure of the DNA dodecamer d(CGCAAATTTGCG)2 complexed with propamidine. *J. Med. Chem.* 38:2317–2325.

Quintana, J. R., A. A. Lipanov, and R. E. Dickerson. 1991. Low-temperature crystallographic analyses of the binding of Hoechst 33258 to the double-helical DNA dodecamer C-G-C-G-A-A-T-T-C-G-C-G. *Biochemistry.* 30:10294–10306.

Schneider, B., K. Patel, and H. M. Berman. 1998. Hydration of phosphate group in double-helical DNA. *Biophys. J.* 75:2422–2434.

Seeman, N. C., J. M. Rosenberg, F. L. Suddath, J. J. P. Kim, and A. Rich. 1976. RNA double-helical fragments at atomic resolution. *J. Mol. Biol.* 104:109–114.

Shatzky-Schwartz, M., N. Arbuckle, M. Eisenstein, D. Rabinovich, A. Bareket-Samish, T. E. Haran, B. F. Luisi, and Z. Shakked. 1997. X-ray and solution studies of DNA oligomers and implications for the structural basis of A-tract-dependent curvature. *J. Mol. Biol.* 267:595–623.

Sherer, E. C., S. A. Harris, R. Soliva, M. Orozco, and C. A. Laughton. 1999. Molecular dynamics on A-tract structure and flexibility. *J. Am. Chem. Soc.* 121:5981–5991.

Shields, G. C., C. A. Laughton, and M. Orozco. 1997. Molecular dynamics simulations of the d(T.A.T) triple helix. *J. Am. Chem. Soc.* 119:7463–7469.

Shui, X., C. C. Sines, L. McFail-Isom, G. G. Hu, and L. D. Williams. 1998. Structure of the potassium form of CGCGAATTCGCG: DNA deformation by electrostatic collapse around inorganic cations. *Biochemistry.* 37:16877–16887.

Simpson, I. J., M. Lee, A. Kumar, D. W. Boykin, and S. Neidle. 2000. DNA minor groove interactions and the biological activity of 2,5-bis-[4-(N-alkylamidino)phenyl] furans. *Bioorg. Med. Chem. Lett.* 10:2593–2597.

Sines, C. C., L. McFail-Isom, S. B. Howerton, D. Vanderveer, and L. D. Williams. 2000. Cations mediate B-DNA conformational heterogeneity. *J. Am. Chem. Soc.* 122:11048–11056.

Spink, N., D. G. Brown, J. V. Skelly, and S. Neidle. 1994. Sequence-dependent effects in drug-DNA interaction: the crystal structure of Hoechst 33258 bound to the d(CGCAAATTTGCG)$_2$ duplex. *Nucleic Acids Res.* 22:1607–1612.

Tabernero, L., N. Verdaguer, M. Coll, I. Fita, G. A. Van der Marel, J. H. Van Boom, A. Rich, and J. Aymami. 1993. Molecular structure of the A-tract DNA dodecamer d(CGCAAATTTGCG) complexed with the minor groove binding drug netropsin. *Biochemistry.* 32:8403–8410.

Tereshko, V., G. Minasov, and M. Egli. 1999a. The Dickerson-Drew B-DNA dodecamer revisited at atomic resolution. *J. Am. Chem. Soc.* 121:470–471.

Tereshko, V., G. Minasov, and M. Egli. 1999b. A ''hydrat-ion'' spine in a B-DNA minor groove. *J. Am. Chem. Soc.* 121:3590–3595.

Vega, M. C., I. Garcia-Saez, J. Aymami, R. Eritja, G. A. Van Der Marel, J. H. VanBoom, A. Rich, and M. Coll. 1994. Three-dimensional crystal structure of the A-tract DNA dodecamer d(CGCAAATTTGCG) complexed with the minor-groove-binding drug Hoechst 33258. *Eur. J. Biochem.* 222:721–726.

Woods, K. K., L. McFail-Isom, C. C. Sines, S. B. Howerton, R. K. Stephens, and L. D. Williams. 2000. Delocalized monovalent cations sequester within the AT-tract minor groove of [d(CGCGAATTC-GCG)]2. *J. Am. Chem. Soc.* 122:1546–1547.

Young, M. A., B. Jayaram, and D. L. Beveridge. 1997a. Intrusion of counterions into the spine of hydration in the minor groove of B-DNA: fractional occupancy of electronegative pockets. *J. Am. Chem. Soc.* 119:59–69.

Young, M. A., G. Ravishanker, and D. L. Beveridge. 1997b. A 5-nanosecond molecular dynamics trajectory for B-DNA: analysis of structure, motions, and solvation. *Biophys. J.* 73:2313–2336.